Molecular Cell, Volume *67*

Supplemental Information

Replication Fork Slowing and Reversal upon DNA Damage Require PCNA Polyubiquitination and ZRANB3 DNA Translocase Activity

Marko Vujanovic, Jana Krietsch, Maria Chiara Raso, Nastassja Terraneo, Ralph Zellweger, Jonas A. Schmid, Angelo Taglialatela, Jen-Wei Huang, Cory L. Holland, Katharina Zwicky, Raquel Herrador, Heinz Jacobs, David Cortez, Alberto Ciccia, Lorenza Penengo, and Massimo Lopes

Replication fork slowing and reversal upon DNA damage require PCNA polyubiquitination and ZRANB3 DNA translocase activity

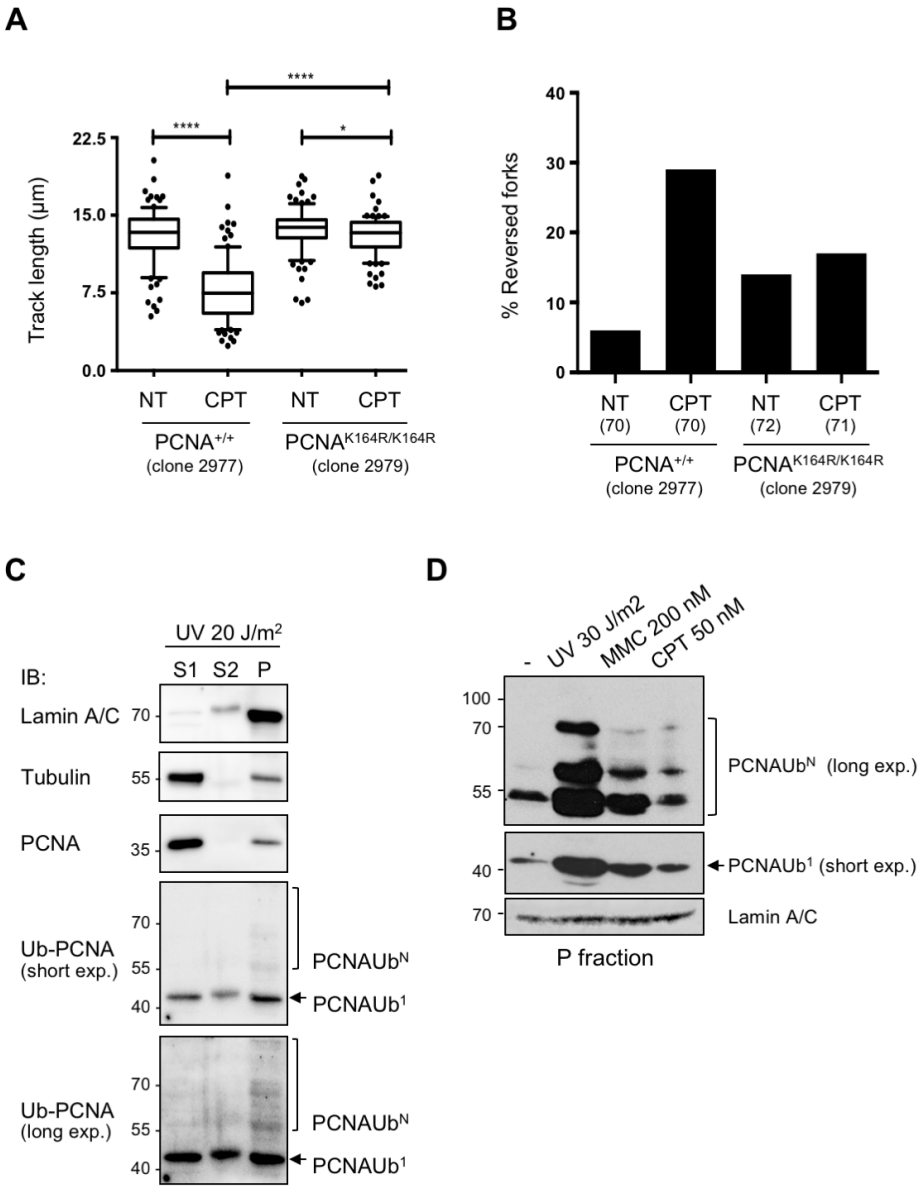

Figure S1, related to Figure 1. A cell fractionation procedure reveals PCNA polyubiquitination in response to acute UV treatment and upon mild CPT or MMC treatments. (A) Control and PCNA-K164R mouse embryonic fibroblasts (MEFs) were subjected to the DNA fiber protocol described in Figure 1A. At least one hundred tracks were scored per sample. Whiskers: 10-90th percentile (***, $P < 0.001$; ns, non-significant, Mann – Whitney test. Similar results were obtained in at least two biological replicates. (B) Frequency of replication fork reversal in the indicated MEFs, upon optional 1h treatment with CPT 50 nM, assessed by *in vivo* psoralen-crosslinking and EM visualization (Zellweger and Lopes, 2017). Similar results were obtained in two biological replicates and in independent MEF clones (Tables S1A-B). (C) Cell fractionation experiment showing the enrichment of ubiquitinated PCNA in fraction P. HCT116 cells were treated with UV irradiation (20 J/m^2) and then subjected to the fractionation protocol detailed in STAR methods. 20 μg of each fraction were loaded onto an SDS-PAGE and analyzed using the indicated antibodies. (D) HCT116 cells were treated with genotoxic treatments (UV 30 J/m^2, MMC 200 nM for 1 h and 50 nM CPT for 1 h). Upon cell fractionation (as in Figure S1C), 70 μg of fraction P were analyzed by immuno-blotting using anti-UbK164PCNA. Lamin A/C is used as loading control. To improve detection of rare PCNA poly-ubiquitinated forms (PCNAUb^N) by UbK164PCNA antibody, the membrane was cut to incubate separately mono-ubiquitinated PCNA (PCNAUb^1, 43 kDa) and the higher molecular weight bands corresponding to the poly-ubiquitinated forms (PCNAUb^N). Two different exposures are shown.

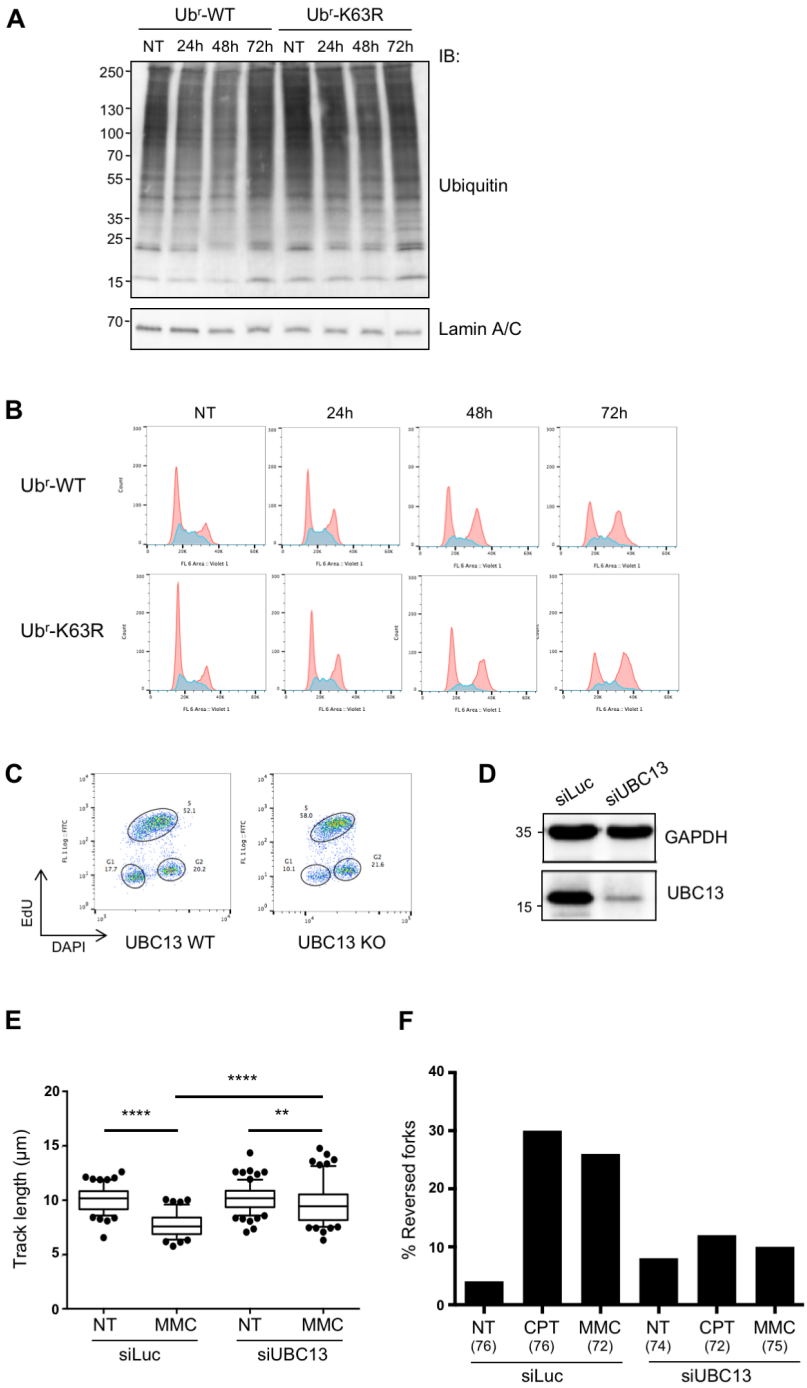

Figure S2, related to Figure 2. UBC13 downregulation in U2OS cells leads to unrestrained replication fork progression and reduced reversed fork frequency upon genotoxic treatments. (A) U2OS cell lines stably carrying either the wild type (Ubr-WT) or the K63R (Ubr-K63R) ubiquitin replacement system (Xu et al, 2009) were treated with doxycycline for different time points to induce the simultaneous knockdown of endogenous ubiquitin and expression of ectopic version. Anti-ubiquitin immunoblotting reveals that - 72h after induction of knowckdown/expression (conditions used in Figure 2A-B) - comparable levels of ubiquitin conjugates are present in Ubr-WT and Ubr-K63R expressing cells. Lamin A/C is used as loading control. (B) Cell cycle distribution analysis by FACS using DAPI for the same cells as in Figure S2A. (C) EdU-DAPI FACS experiment showing marginal differences in cell cycle distribution, between wild type (WT) or UBC13 knock out (KO) HCT116 cells (see Figure 2). (D) Western Blot showing efficiency of siRNA-mediated UBC13 downregulation in U2OS cells. GAPDH, loading control. (E) Control (siLuc) or UBC13-depleted (siUBC13) U2OS cells were subjected to the DNA fiber protocol as in Figure 1A upon optional mitomycin C (200 nM) treatment. At least one hundred tracks were scored per sample. Whiskers: 10-90th percentile (****, $P < 0.0001$; **, $P < 0.05$; Mann – Whitney test). Very similar results were obtained in at least two biological replicates. (F) Frequency of replication fork reversal in control (siLuc) or UBC13-depleted (siUBC13) U2OS cells, assessed by in vivo psoralen-crosslinking and EM visualization, upon optional 1h treatment with CPT 50 nM or MMC 200 nM. In brackets, the number of analyzed molecules. Very similar results were obtained in two biological replicates (Table S2C).

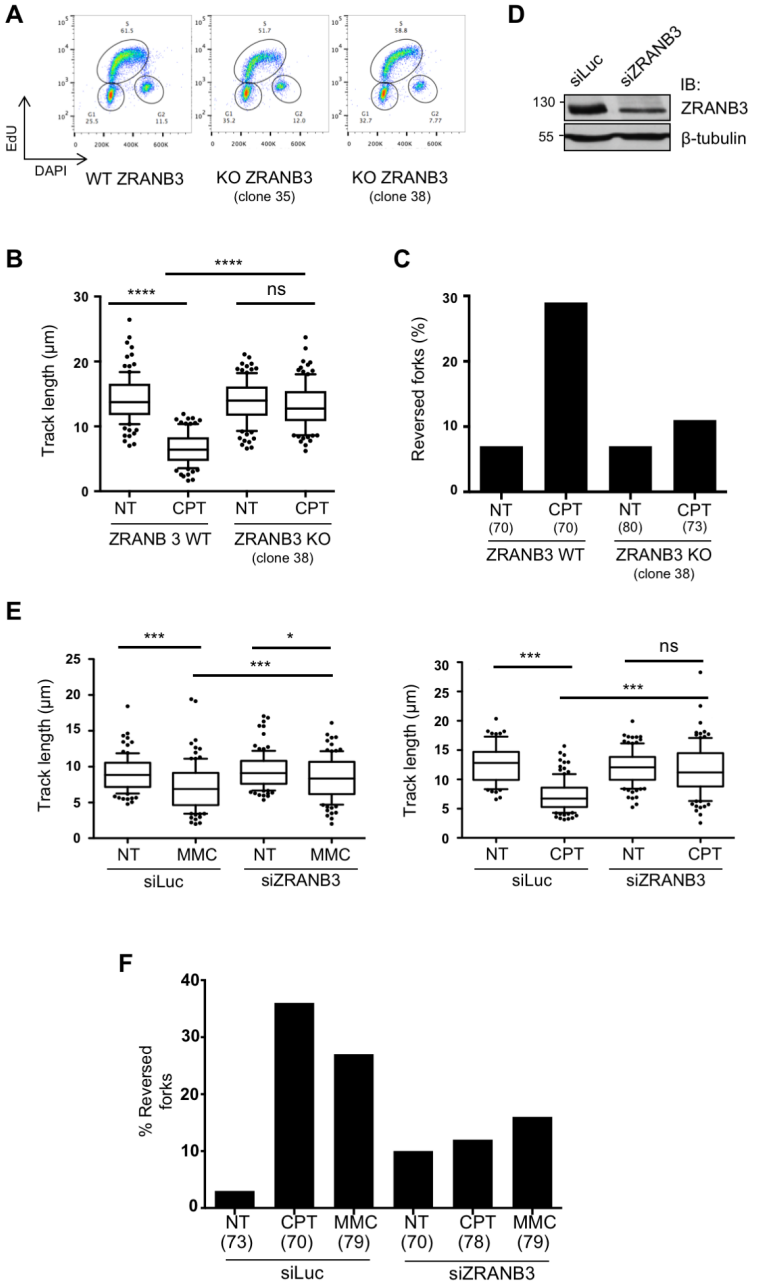

Figure S3, related to Figure 3. ZRANB3 downregulation in U2OS cells leads to unrestrained replication fork progression and reduced reversed fork frequency upon genotoxic treatments. (A) EdU-DAPI FACS experiment showing marginal differences in cell cycle distribution, between wild type (WT) or ZRANB3 knock out (KO) U2OS clones (see Figure 3 and Figure S3B-S3C). (B) Wild type (WT) or ZRANB3-knock-out (ZRANB3-KO) U2OS cells were subjected to the DNA fiber protocol in Figure 1A. At least one hundred tracks were scored per sample. Whiskers: 10-90th percentile (****, $P < 0.0001$; ns, non-significant, Mann – Whitney test). Similar results were obtained in at least two biological replicates. (C) Frequency of replication fork reversal in WT and ZRANB3-KO U2OS cells, assessed by in vivo psoralen-crosslinking and EM visualization, upon optional 1h treatment with CPT 50 nM. In brackets, the number of analyzed molecules. Similar results were obtained in two biological replicates and in two independent ZRANB3-KO clones (Tables S3A-B). (D) Western Blot showing efficiency of siRNA-mediated ZRANB3 downregulation in U2OS cells. β tubulin, loading control. (E) Control (siLuc) or ZRANB3-depleted (siZRANB3) U2OS cells were subjected to the DNA fiber protocol as in Figure 1A, upon optional treatments with MMC 200 nM (left) or CPT 50 nM (right). At least one hundred tracks were scored per sample. Whiskers: 10-90th percentile (****, $P < 0.0001$; *, $P < 0.5$; Mann – Whitney test). Very similar results were obtained in at least two biological replicates. (F) Frequency of replication fork reversal in control (siLuc) or ZRANB3-depleted (siZRANB3) U2OS cells, assessed by in vivo psoralen-crosslinking and EM visualization, upon optional 1h treatment with CPT 50 nM or MMC 200 nM. In brackets, the number of analyzed molecules. Very similar results were obtained in two biological replicates (Table S3C).

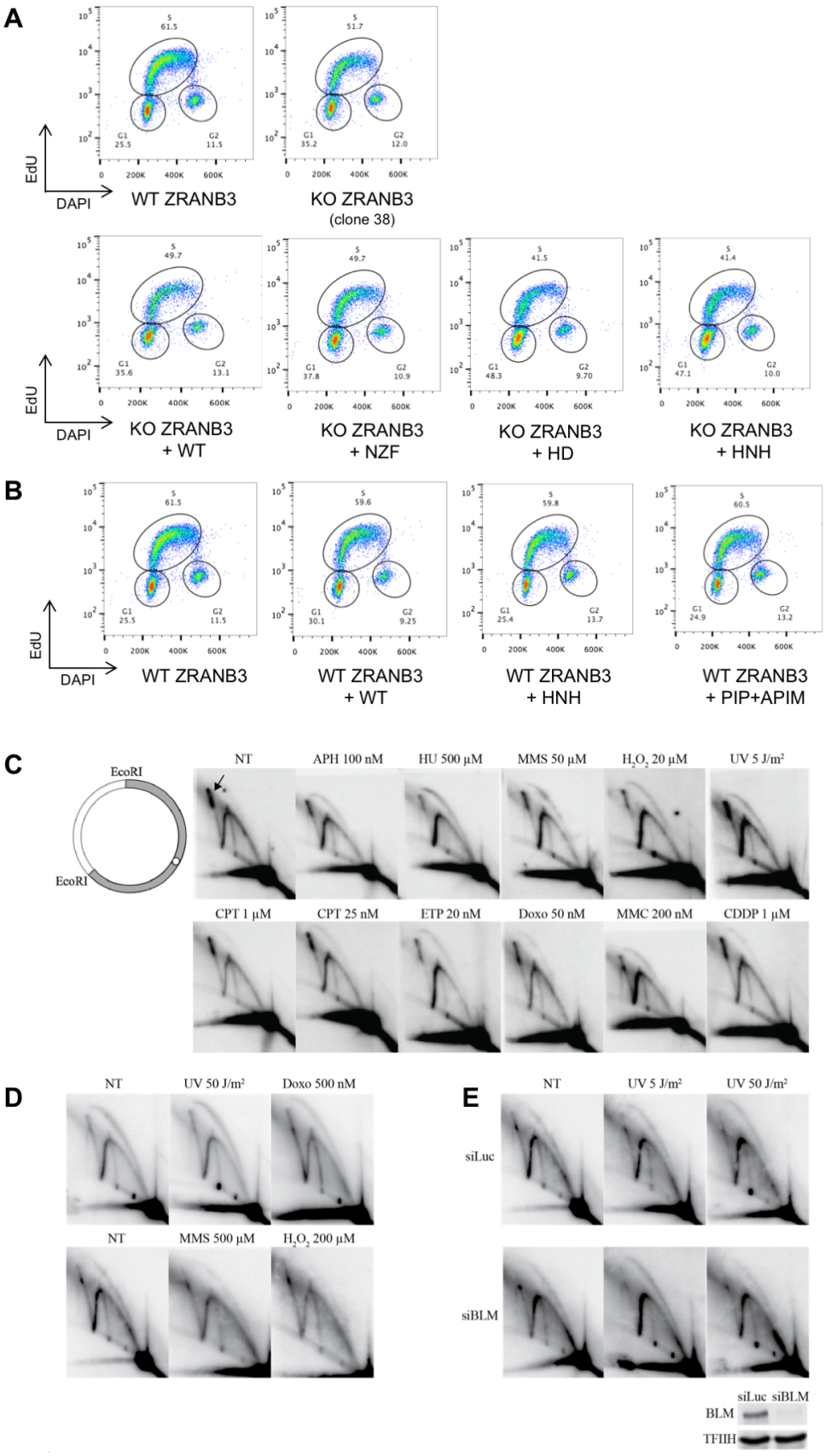

Figure S4, related to Figure 4. See next page.

Figure S4, related to Figure 4. (A-B) EdU-DAPI FACS analysis of cell lines stably expressing HA-ZRANB3 WT or mutant protein. FACS analysis of EdU-incorporation and DAPI illustrating marginal differences in cell cycle distribution among stable cell lines derived from U2OS ZRANB3 KO cell lines (A) and ZRANB3 WT cell lines (B), upon complementation with WT or mutant HA-ZRANB3 (see Figure 4). (C-E) Acute genotoxic treatments and genetic impairment of joint-molecule dissolution do not lead to detectable accumulation of post-replicative sister-chromatid junctions in human cells. Rationale: Depending on repair/replication kinetics and lesion type, cells can tolerate DNA impediments at or behind the replication fork. Lesion bypass at the fork is achieved by switching to a translesion synthesis polymerase (TLS) or by template switching through fork reversal. Single strand gaps behind the fork can be sealed by TLS or by template switching via post-replicative junctions. In Saccharomyces cerevisiae, post-replicative template switching has been extensively studied. X-shaped structures representing post-replicative junctions accumulate in specific genetic conditions, in particular upon impairment of their dissolution by deletion of the yeast RecQ helicase Sgs1 (Branzei et al., 2006; Liberi et al., 2005). Using high-copy number linear minichromosomes, these X-shaped structures were selectively isolated from 2D gels and studied by TEM (Giannattasio et al., 2014). Data: To visualize post-replicative junctions in human cells, we took advantage of an SV40-based episomal system that replicates with very high efficiency and allows isolation of in vivo replication intermediates (Follonier and Lopes, 2014; Follonier et al., 2013). However, neither low (C) nor high (D) dose of various genotoxic treatments did induce detectable accumulation of X-shaped structures, over levels usually detected in untreated cells (arrow). (E) Furthermore, X-shaped structures did not accumulate after downregulation of the human Sgs1 homolog Bloom syndrome protein (BLM), which has been shown to dissolve sister chromatid junctions in human cells (Wu and Hickson, 2003). These data strongly suggest that, contrary to yeast, template switching in human cells occurs primarily at the replication for via fork reversal, which is indeed very abundantly detected and dependent upon error-free PRR factors (see main text). Method: Neutral-neutral 2D-gel analysis of plasmid pML113 transfected into untreated (NT) HEK-293T cells and upon 1 h treatment with the indicated dose of genotoxic drugs. Plasmid was recovered after 40 h and digested by EcoRI as indicated. 2D gel analysis was performed as described (Follonier and Lopes, 2014); the probe reveals replication intermediates in the gray fragment (top left scheme; circle, SV40 replication origin). APH=Aphidicolin, HU=Hydroxyurea, MMS=Methyl Methanesulfonate, H2O2=Hydrogen Peroxide, UV=UV-C irradiation, CPT=Camptothecin, ETP=Etoposide, Doxo=Doxorubicin, MMC=Mitomycin C, CDDP=Cisplatin. Bloom (BLM) levels after siRNA-mediated depletion were detected by immunoblotting. TFIIH, loading control.

A

MEF	WT (clone 2976)	WT (clone 2976)	WT (clone 2976)	PCNA^{K164R} (clone 2978)	PCNA^{K164R} (clone 2978)	PCNA^{K164R} (clone 2978)
CPT	-	+	-	-	+	-
MMC	-	-	+	-	-	+
% RF Exp #1	4 (75)	29 (92)	26 (87)	12 (75)	11 (79)	10 (80)
% RF Exp #2	9 (79)	30 (79)	23 (92)	11 (85)	13 (80)	16 (106)

B

MEF	WT (clone 2977)	WT (clone 2977)	PCNA^{K164R} (clone 2979)	PCNA^{K164R} (clone 2979)
CPT	-	+	-	+
% RF Exp #1	6 (70)	29 (70)	14 (72)	17 (71)
% RF Exp #2	6 (70)	30 (73)	12 (73)	19 (74)

Table S1, related to Figure 1. Electron microscopy data for experiments in Figures 1D and S1B.
(A) Percentage of observed reversed forks (% RF) in two independent EM experiments for samples in Figure 1D.
(B) Percentage of observed reversed forks (% RF) in two independent EM experiments for samples in Figure S1B.
Number of analyzed molecules in brackets.

A

U2OS Ub^{r}-system	WT	WT	WT	K63R	K63R	K63R
CPT	-	+	-	-	+	-
MMC	-	-	+	-	-	+
% RF Exp #1	10 (72)	32 (70)	26 (75)	9 (71)	12 (73)	13 (72)
% RF Exp #2	8 (82)	29 (74)	25 (77)	9 (70)	17 (73)	13 (70)

B

HCT116 UBC13 WT/KO	WT	WT	WT	WT	KO	KO	KO	KO
CPT	-	+	-	-	-	+	-	-
MMC	-	-	+	-	-	-	+	-
UV	-	-	-	+	-	-	-	+
% RF Exp #1	5 (70)	28 (73)	23 (79)	23 (72)	8 (71)	11 (71)	12 (71)	11 (71)
% RF Exp #2	5 (71)	27 (87)	21 (91)	21 (75)	8 (74)	11 (81)	11 (71)	11 (72)

C

U2OS	siluc	siluc	siluc	siUBC13	siUBC13	siUBC13
CPT	-	+	-	-	+	-
MMC	-	-	+	-	-	+
% RF Exp #1	4 (76)	30 (76)	26 (72)	8 (74)	12 (72)	10 (75)
% RF Exp #2	4 (75)	29 (92)	26 (86)	12 (75)	11 (79)	10 (80)

Table S2, related to Figure 2. Electron microscopy data for experiments in Figures 2B, 2E and S2F.
(A) Percentage of observed reversed forks (% RF) in two independent EM experiments for samples in Figure 2B.
(B) Percentage of observed reversed forks (% RF) in two independent EM experiments for samples in Figure 2E.
(C) Percentage of observed reversed forks (% RF) in two independent EM experiments for samples in Figure S2F.
Number of analyzed molecules in brackets.

A

U2OS ZRANB3 WT/KO	WT	WT	WT	WT	KO (clone 35)	KO (clone 35)	KO (clone 35)	KO (clone 35)
CPT	-	+	-	-	-	+	-	-
MMC	-	-	+	-	-	-	+	-
UV	-	-	-	+	-	-	-	+
% RF Exp #1	5 (71)	28 (78)	21 (75)	20 (77)	6 (74)	13 (77)	12 (71)	3 (74)
% RF Exp #2	6 (74)	30 (71)	22 (70)	20 (71)	7 (70)	15 (73)	11 (74)	9 (72)

B

U2OS ZRANB3 WT/KO	WT	WT	KO (clone 38)	KO (clone 38)
CPT	-	+	-	+
% RF Exp #1	7(70)	29 (70)	7 (80)	11 (73)
% RF Exp #2	7(75)	27 (76)	7 (71)	11 (70)

C

U2OS	siluc	siluc	siluc	siZRANB3	siZRANB3	siZRANB3
CPT	-	+	-	-	+	-
MMC	-	-	+	-	-	+
% RF Exp #1	4 (73)	35 (70)	26 (79)	10 (70)	12 (78)	14 (79)
% RF Exp #2	6 (71)	31 (79)	25 (76)	9 (81)	14 (71)	12 (70)

Table S3, related to Figure 3. Electron microscopy data for experiments in Figures 3C, S3C and S3F.
(A) Percentage of observed reversed forks (% RF) in two independent EM experiments for samples in Figure 3C.
(B) Percentage of observed reversed forks (% RF) in two independent EM experiments for samples in Figure S3C.
(C) Percentage of observed reversed forks (% RF) in two independent EM experiments for samples in Figure S3F.
Number of analyzed molecules in brackets.

U2OS ZRANB3 KO (clone 35) - complementation	WT	WT	PIP/APIM	PIP/APIM	NZF-zinc	NZF-zinc
CPT	-	+	-	+	-	+
% RF Exp #1	5 (71)	32 (70)	8 (76)	12 (83)	8 (73)	12 (71)
% RF Exp #2	6 (76)	30 (72)	9 (72)	12 (74)	10 (73)	12 (73)

U2OS ZRANB3 KO (clone 35) - complementation	WT	WT	HD	HD	HNH	HNH
CPT	-	+	-	+	-	+
% RF Exp #1	5 (72)	29 (73)	5 (72)	5 (73)	5 (97)	31 (70)
% RF Exp #2	4 (75)	28 (70)	5 (94)	5 (70)	6 (70)	26 (86)

Table S4, related to Figure 4. Electron microscopy data for experiments in Figure 4C.
Percentage of observed reversed forks (% RF) in two independent EM experiments for samples in Figure 4C. Number of analyzed molecules in brackets.